Nanolithographically defined magnetic structures and quantum magnetic disk (invited)

Stephen Y. Chou, Peter R. Krauss, and Linshu Kong
NanoStructure Laboratory, Department of Electrical Engineering, University of Minnesota, Minneapolis, Minnesota 55455

Isolated and interactive arrays of magnetic nanostructures as small as 15 nm are fabricated using nanolithography and related technologies, and are characterized using magnetic force microscopy. It has been demonstrated that manipulating the size, aspect ratio, and spacing of these nanostructures can lead to unique control of their magnetic properties. A quantum magnetic disk based on discrete single-domain nanomagnetic structures with storage density of 65 Gbits/in.^{2} is demonstrated along with a low-cost method for mass producing such disks. Other impacts that nanofabrication can bring to the development of future magnetic storage are discussed. © *1996 American Institute of Physics.* [S0021-8979(96)41908-8]

I. INTRODUCTION

In the epic of information and multimedia, there are increasing demands for magnetic storage devices with higher density, faster speed, lower power consumption, smaller size, and lower weight than the current state-of-the-art devices. Presently, most magnetic storage devices are based on the properties of magnetic thin films. Therefore, enormous research efforts have been devoted to the study and control of the key factors that affect magnetic thin film properties.[1–4] These factors include the size and shape anisotropy of the grains in the film, the grain magnetization orientation, the spacing and coupling between the grains, and material compositions.

The advent of nanofabrication technology opens up new avenues to manipulate magnetic materials, thereby leading to unique opportunities in developing innovative ultrahigh density magnetic storage, engineering new magnetic materials and devices, and obtaining better understanding of micro-magnetics. Nanofabrication can make magnetic structures with dimensions comparable to or smaller than some fundamental length scales in magnetics, such as domain wall size and exchange interaction length, thus making the behavior different from that of a thin film. Nanofabrication can create arrays of interactive magnetic nanoparticles with precisely controlled interparticle spacing. Nanofabrication can arrange the orientation and position of the nanoparticles at one's will. With such unique manipulation ability offered by nanotech-nology, many revolutionary device concepts are no longer regarded as ''wild dreams,'' but become reality.

This article reviews research on nanomagnetic structures fabricated using electron-beam lithography and other fabrication technologies carried out at the NanoStructure Laboratory at the University of Minnesota. Particularly, this article will discuss (1) fabrication and characterization of isolated and interactive single-domain magnetic nanostructures such as bars, pillars, and rings, and (2) properties and low-cost fabrication of a 65 Gbits/in.^{2} quantum magnetic disk—a new paradigm for ultrahigh density magnetic recording media with a recording density two orders of magnitude greater than current state-of-the-art disks. The work done elsewhere on lithographically defined magnetic structures can be found in Refs. 5–8.

II. FABRICATION OF MAGNETIC STRUCTURES USING NANOLITHOGRAPHY

A typical fabrication process is illustrated in Fig. 1. In the fabrication, a resist film, polymethylmethacrylate (PMMA), is first spun onto a substrate, typically silicon. A high resolution electron beam lithography system is used to expose patterns in the PMMA.[9] The exposed PMMA is developed in a cellosolve and methanol solution to form a resist template on the substrate. Ferromagnetic materials can be patterned using either a lift-off or electroplating process. In a lift-off process, a ferromagnetic metal film is first deposited onto the entire sample. The sample is then immersed in acetone that dissolves the PMMA template and lifts off the metal on the PMMA surface, but not the metal on the substrate. In an electroplating process, a thin metal plating base is placed between the PMMA and the substrate, and the PMMA template is removed after plating. Besides use for lift-off and plating, the PMMA template also can be used to etch nanostructures into the substrate that will be used later to create magnetic nanostructures.

Figures 2–4 show scanning electron microscope (SEM) images of three magnetic nanostructures fabricated using nanolithography and a lift-off process.[10,11] The nanostruc-tures are a high aspect ratio, isolated Ni bar 15 nm wide and 1 μm long, an interactive Ni bar array of 20 nm wide and 200 nm long bars, and Ni rings with a 90 nm mean diameter

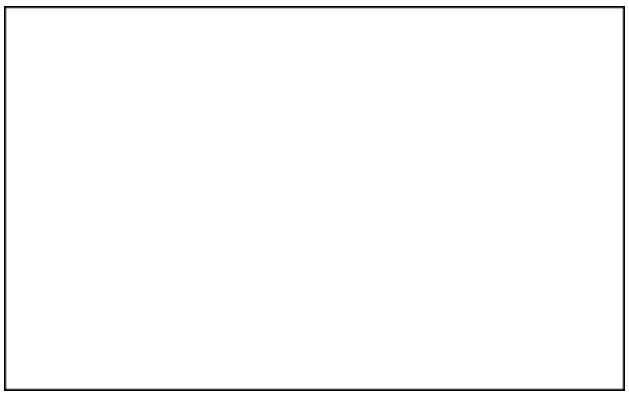

FIG. 1. Schematic of a typical process for fabricating nanomagnetic structures using nanolithography and related technologies.

J.
Appl. Phys. **79** (8), 15 April 1996 0021-8979/96/79(8)/6101/6/$10.00

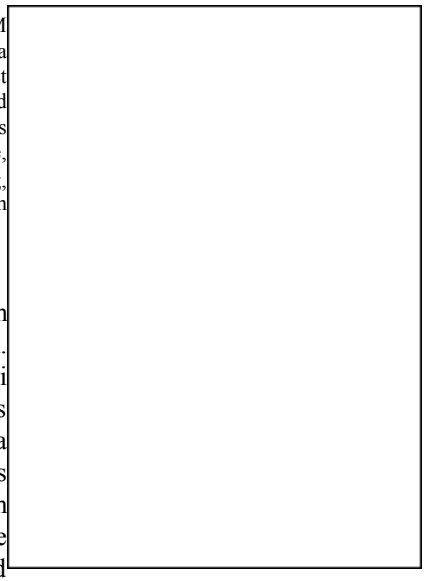

FIG. 2. SEM image of a high aspect ratio isolated Ni bar that is 15 nm wide, 1 p.m long, and 35 nm thick.

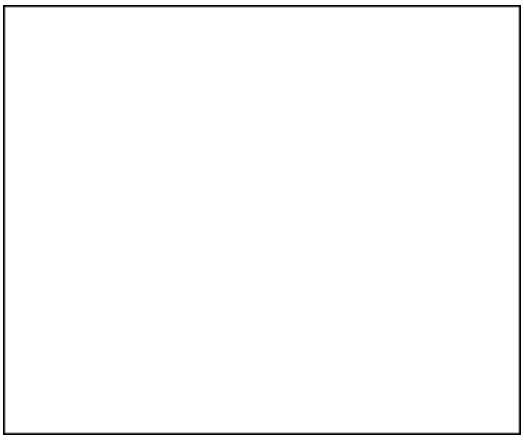

FIG. 4. SEM image of Ni rings of a 90 nm mean diameter, 25 nm ring width, and 35 nm thickness on Si.

and 25 nm ring width. The Ni structures have a thickness of 35 nm and were fabricated on a Si substrate. Figure 5 shows a SEM image of a Ni pillar array with 100 nm spacing, 75 nm average diameter, 700 nm height, and therefore 9.3 aspect ratio fabricated using nanolithography and electroplating.[12]

III. PROPERTIES OF NANOMAGNETIC STRUCTURES

The first striking property of nanolithographically defined magnetic structures is that without an applied magnetic field, each structure can magnetize itself, making the magnetic moments of all polycrystalline grains in the structure align to the same direction. The single-domain formation is due to the fact that the magnetostatic energy in these magnetic nanostructures is lower than the domain wall energy. magnetization to be aligned along the long axis of the bars and pillars. This single-domain formation and alignment make the magnetic moment quantized with only two stable states, equal in magnitude but opposite in direction. Figure 6 shows that when examined using magnetic force microscopy, each nickel bar, which is 100 nm wide, 35 nm thick, and 1 iLm long, has two opposite magnetic poles at the ends of the bar and no poles in between—a clear picture of a single magnetic domain element.

The second property is that the magnetic field needed to switch the magnetization of a single-domain element from one direction to the opposite direction can be controlled by changing the geometry of the structure, such as bar's width, length, and thickness. Figure 7 shows that the switching field of nickel and cobalt bars with a 1μm length and 35 nm thickness increases as the width of the bar decreases. The peak switching fields are 740 Oe for Ni and 3000 Oe for Co, respectively, which are over 30 times larger than the switching field of the as-deposited films.[11,13]

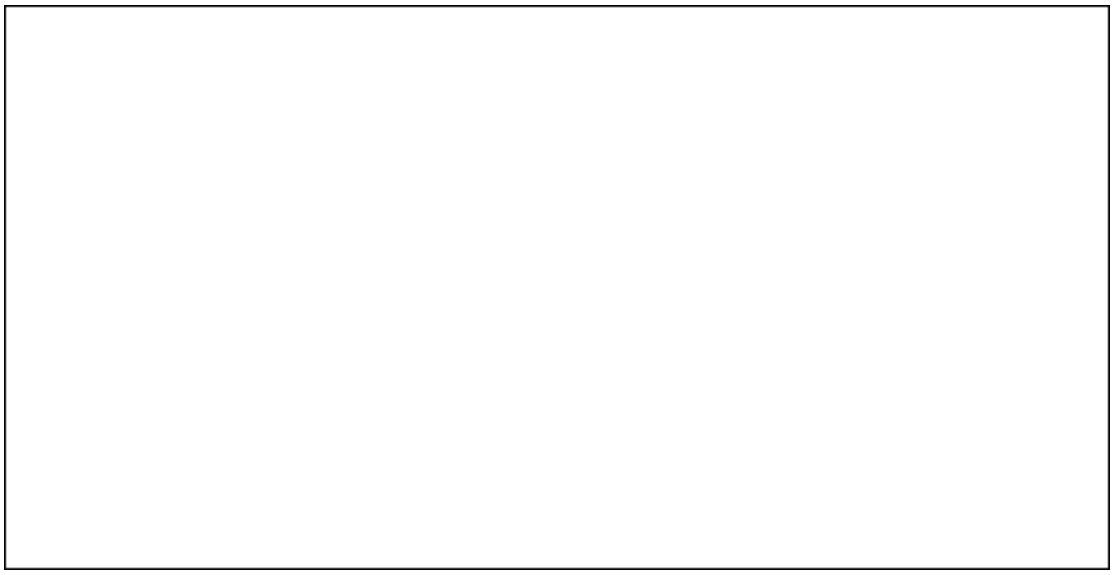

FIG. 3. SEM image of an interactive Ni bar array. Each bar is 20 nm wide, 200 nm long, and 35 nm thick.

FIG. 5. SEM image of Ni pillar array of a 100 nm spacing, 75 nm average diameter, 700 nm height, and therefore 9.3 aspect ratio.

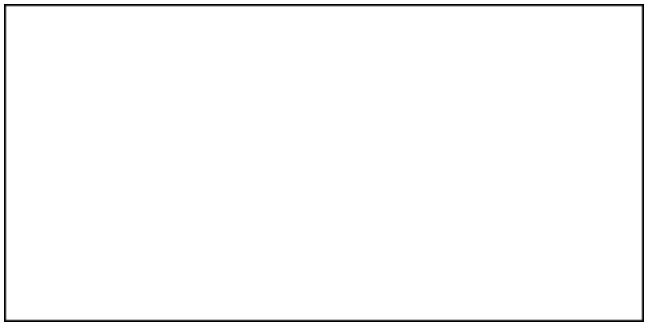

FIG. 6. The atomic force microscopy (a) and magnetic force microscopy (b) of three single-domain nickel bars that are 100 nm wide, 1 μm long, and 35 nm thick.

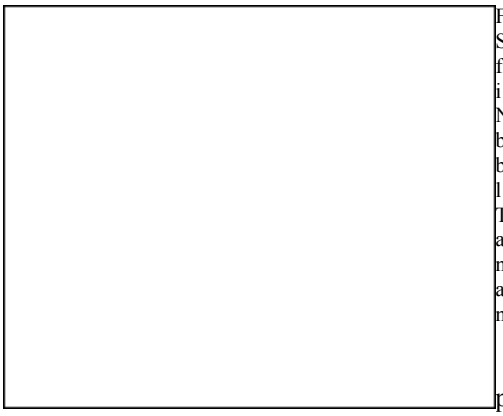

FIG. 8. Switching field of isolated Ni and Co bars vs bar length. The bars are 100 nm wide and 35 nm thick.

further controlled by varying the bar length as shown in Fig. 8. It was found that the length dependence is nonmonotonic.[13] The switching field increases with the bar length initially, but then decreases after reaching a peak. For isolated nickel and cobalt bars with a thickness of 35 nm and a width of 100 nm, the peak switching field and corresponding bar length are, respectively, 640 Oe and 1 μm for Ni, and 1250 Oe and 2 μm for Co. Moreover, it was observed that the decrease of the switching field with the increase of the bar width is much faster in Ni bars than in Co bars. These results suggest that quasi-coherent switching occurs in short bars and incoherent switching occurs in long bars, and that the exchange coupling is much stronger in Co bars than that in Ni bars.

The effects of the magnetostatic field of a single-domain bar on the crystalline anisotropy and the switching field of its neighbors were studied using nanolithography technology.[14] In this study, pairs of single-domain cobalt bars that were 35 nm thick, 50 nm wide, 1 μm long and with a spacing from 50 to 1000 nm, were fabricated using electron-beam lithography and a lift-off process. Magnetic force microscopy was used to study the switching behavior of one bar in the presence of another bar and the intrinsic switching field of one bar after the other bar was physically removed. Figure 9 shows the measured switching field for the three cases: (a) only one of the twin bars is switched, H_{TI}; (b) both bars are switched, H_{TT}; (c) one bar switched after the other bar was physically removed by a nanotechnique, H_T. One of the key findings is that even after the neighboring bar was physically removed, the intrinsic switching field of one bar still strongly depends on the original spacing between the bars. Also, the smaller the bar spacing was, the larger the intrinsic switching field. This is attributed to the spontaneous formation of a single-domain region during the Co deposition, whose mag-netostatic field enhances the crystalline anisotropy of its neighbors. These results suggest that during the deposition of magnetic media, substrate roughness and large in-plane shape anisotropy of magnetic grains will strongly affect the magnetic properties of neighboring grains and therefore the uniformity of the disk.

Finally, ferromagnetic rings were studied using MFM. It was found that for the rings with a diameter 500 nm or less, no magnetic poles can be observed, indicating the rings are a single domain.

IV. QUANTUM MAGNETIC DISK

As data storage densities reach 500 MBits/in.^{2} in commercial magnetic hard disks and 3 Gbits/in.^{2} in the most advanced laboratory disks, it becomes apparent that one of

FIG. 7. Switching field of isolated Ni and Co bars vs bar width. The bars are 1 μm long and 35 nm thick. The actual bar width was measured using SEM.

FIG. 9. Switching field of twin single-domain Co bars vs the bar spacing H_{π}, only one of twin bars is switched; $H_{\uparrow\uparrow}$, both bars are switched; H_{τ}, switching field after one of the twin bars was removed.

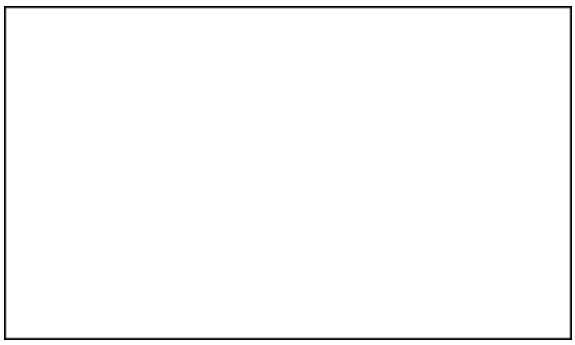

FIG. 10. Schematic of a quantum magnetic disk which consists of pre-patterned single-domain magnetic structures embedded in a nonmagnetic disk. Only the vertical magnetization is shown, but the disk can be made with longitudinal magnetization.

the key factors that limit the storage density is the nature of magnetic thin films that are used as the recording media. Many of the limitations can be readily removed if each bit is stored in a discrete magnetic element that is separated from its neighbors by a nonmagnetic material. More advantages can be obtained if each element is made of a single magnetic domain. These ideas are the basis for a new magnetic recording paradigm, the quantum magnetic disk.

A quantum magnetic disk (QMD) completely abandons the continuous magnetic thin film as the recording media used in the conventional disk. Instead, the QMD uses prefabricated discrete single-domain magnetic elements uniformly embedded in a nonmagnetic disk, as shown in Fig. 10.[11] Each element has a uniform and well-defined shape, a pre-specified location, and most importantly, a quantified magnetization that has only two states, identical in magnitude but opposite in direction. Each element can store a bit of binary information. The other striking property is that the magnetic field needed for switching the magnetization direction of the elements can be controlled by engineering the elements' geometry.

Before discussing the unique advantages of QMDs in writing, reading, and tracking, let us look at the fabrication process and properties of one QMD embodiment that consists of single-domain nickel (magnetic) nanopillars uniformly embedded in a SiO_2 (nonmagnetic) disk.[15,16] In fabrication, electron-beam lithography was used to define the QMD bit's size and location, and reactive ion etching was used to drill holes in the SiO_2 layer carried on a Si substrate. Nickel electroplating was used to selectively deposit nickel into the holes and chemical mechanical polishing was used to planarize the surface.

The properties of the QMD have been investigated using scanning electron microscopy (SEM), tapping mode atomic force microscopy (TMAFM), and magnetic force microscopy (MFM).[16] A SEM micrograph of a 3 bit by 3 bit section of the QMD in a top view is shown in Fig. 11(a). The micrograph shows that the nickel pillars of the QMD have a 50 nm diameter and a 100 nm period. The pillars are 200 nm tall and thus have an aspect ratio of 4.

TMAFM and MFM images taken simultaneously on the same area of the QMD are shown in Figs. 11(b) and 11(c), respectively. The TMAFM image of a 3 bit by 3 bit section of the QMD shows that the topology of the nickel pillars is indistinguishable from that of the SiO_2. The surface is very smooth with a roughness of 0.5 nm root-mean-squared. The corresponding MFM image, on the other hand, clearly shows that each bit has a quantized magnetization orientation and the magnetic image of each pillar of the 9 bit section can be resolved. Five bits have the south pole (bright) on the top surface and the other four bits have the north pole (dark) on the top. The QMD was demagnetized before imaging, therefore the nearest neighbor bits have opposite magnetic directions. This magnetization configuration is the lowest energy state for the QMD. Our study also showed that the nickel pillar can be switched using a MFM tip with a large magnetic moment. The storage density of the QMD is 65 Gbits/in.^{2}, which is over two orders of magnitude higher than that of state-of-the-art commercial magnetic disks.

The advantages of quantum magnetic disks over the conventional disks are apparent. First, the writing process in the quantum disk is simplified and becomes quantized, resulting in much lower noise and lower error rate and allowing much higher density. Instead of precisely defining the magnetic moment, area, and location of each bit as in a conventional magnetic disk, the writing process in a QMD simply requires flipping the magnetization direction of a discrete single-domain bit. Micromagnetics simulation has shown that even if a writing field is smaller than the size of the bit, the writing field will flip the magnetization direction of the entire bit, leading to a perfect writing.[17] Furthermore, simulation has shown that if the overlap between the writing field and a bit is insignificant, the writing field would only temporarily perturb the magnetic moment distribution of the bit. When the writing field is removed from the bit, the magnetic moment of the bit returns to its original state. In other words, the writing process in a QMD is quantized: a write head either writes perfectly the entire bit, or it does not write the bit at all. The quantized writing process in the QMD will allow the use of a smaller and therefore faster write head. It will avoid errors due to the misplacement and the fringing field of the wire head, and hence is suitable for ultrahigh density storage.

The second advantage of the QMD is near zero transition noise. The transition region between two bits is replaced by a nonmagnetic material and the grains in a QMD bit are tightly coupled and behave like a single large grain. As a result, the noise from the fluctuation of grain magnetization orientation should be greatly reduced, if not completely eliminated. In QMDs, the boundaries between the bits are defined by lithography and etching. They can be very smooth, giving quiet reading signals.

The third advantage of the QMD is reduced cross talk between bits. The cross talk in conventional disks comes from the interbit exchange interaction and magnetostatic interactions. In QMDs, by replacing the ferromagnetic material that is between the bits with a nonmagnetic material, the exchange interaction between the bits gets cut off completely and the interbit magnetostatic interaction is greatly reduced.

The fourth advantage is a solution to the tracking problem. In conventional magnetic disks, the bits do not always have physically recognizable boundaries between them.

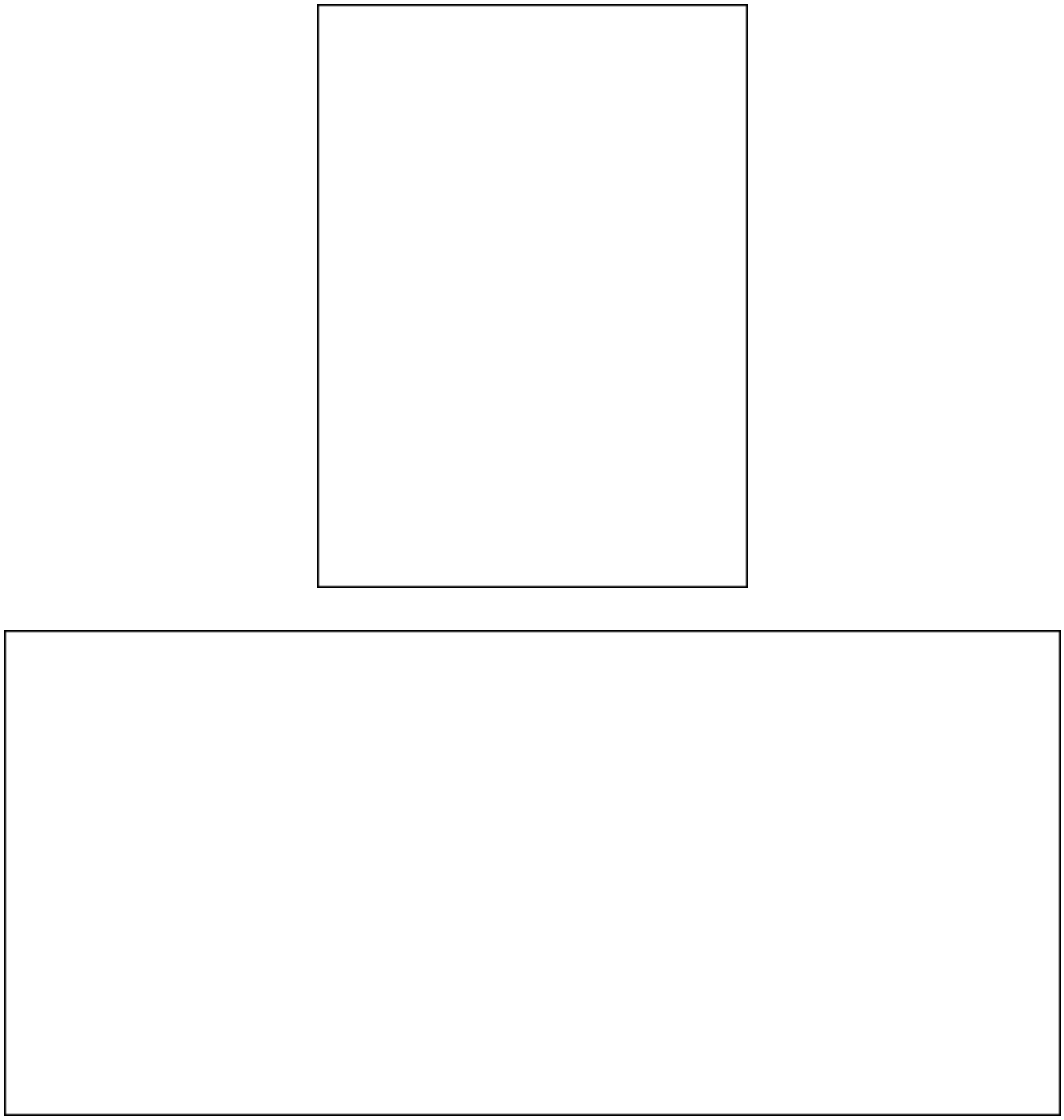

FIG. 11. (a) SEM image, (b) TMAFM image, and (c) MFM image of 3 by 3 bits of a QMD with 65 Gbits/in.^{2} density. Each bit consists of a nickel pillar uniformly embedded in 200 nm SiO_2 with a 50 nm diameter (aspect ratio of 4) and a 100 nm period. The TMAFM image shows a very smooth surface with a roughness of 0.5 nm rms. The MFM image shows an alternating pattern of magnetization directions from each bit.

Tracking depends on the writing of the tracking marks and the ability to rotate the disk the exact amount so that the desired data aligns with the head that writes or reads it. In other words, the tracking is ''blind.'' Furthermore, over 14% of total disk area is used to write the tracking marks in current commercial disks. The area for tracking marks is expected to take up significantly more disk area in future high density disks where more precise tracking is required. In the QMDs, each bit is isolated from one another by nonmagnetic material. Therefore, there is always a variation of magnetic field between the bits (regardless of their magnetization directions) that provides the signal for actual tracking of each bit. Namely, in a QMD drive, each bit can be physically seen before writing or reading.

Clearly, to make the QMDs a competitive technology, low-cost mass production methods must be developed. One of the very promising technologies that we have developed is the nanoimprint lithography which replaces *e*-beam nanolithography.[18] In nanoimprint lithography, a mold is first made with the nanoscale features. Then it is pressed into a resist to create a thickness contrast pattern. After removing the mold, the pattern will be transferred into the entire resist by RIE. A SEM micrograph of 25 nm diam metal dots fabricated by nanoimprint lithography and lift-off is shown in Fig. 12.

From the above discussion, it is clear that the QMD differs from the discrete track disk[19,20] and the discrete segment disk.[21,22]

Finally, we would like to point out that although development of QMDs is still in its infancy, great interest has been generated. Our research shows that with the state-of-the-art nanofabrication technology, the density of QMDs can reach a

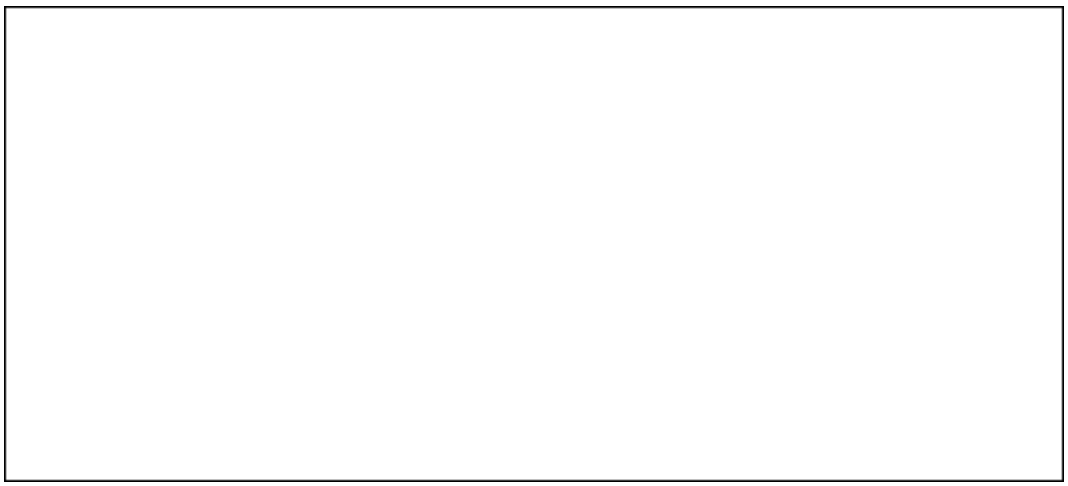

FIG. 12. SEM image of 25 nm diameter metal dots fabricated by nanoim-print lithography and lift-off.

FIG. 13. SEM image of a metal dot array with a density of 0.25 Tbits/in.^{2}

0.25 Tbits/in.^{2} (Fig. 13) and yet each bit is thermally stable. Besides the QMD media, the future development of the QMDs involves the development of the ultrahigh resolution, high-speed read and write heads as well as new drive systems. The heads will very likely utilize the advanced technologies of nanofabrication and scanning force probes. They will be in the form of large parallel arrays. The disk drive may deviate from the classic circular geometry; instead it may be a linear drive based on state-of-the-art microme-chanical elements. Because of the ultrahigh density offered in the QMDs, the total disk area for a 30 Gbit disk can be well less than the size of a penny.

V. CONCLUSION

Using nanolithography based fabrication technology, magnetic structures can be engineered to have magnetic properties that cannot be achieved by conventional methods. Undoubtedly, the nanofabrication approach opens up new opportunities for engineering novel magnetic materials, understanding the fundamentals of magnetics, exploring limits of magnetic storage, and developing ultrahigh density magnetic storage and innovative magnetic devices such as read and write heads for hard disks, magnetotransport devices, and magneto-optical devices.

ACKNOWLEDGMENTS

It gives us great pleasure to thank many past and current members of NanoStructure Lab at the University of Minnesota who have contributed significantly to the magnetic nanostructures and quantum magnetic disk projects; in particular, Mark Wei for his study of single-domain elements, Usman Suriono for micromagnetics simulation, Preston Ren-strom for his assistance in developing the nanoimprinting technology, and Dr. Paul Fischer and Robert Guibord for their technical assistance in fabrication. We are also grateful to Professor J. G. Zhu for stimulating discussion. This work was partially supported by Office of Naval Research, Advanced Research Program Agency, and a Packard Fellowship. The magnetic force microscope is supported by Army Research Office through a DURIP.

[1]For example, M. Kryder, 40th MMM Conf., 1995 and the proceedings of MMM Conf. and Intrmag.
[2]A. Aharioni, J. Appl. Phys. **63**, 5879 (1988).
[3]Y. Martin and H. K. Wickramasinghe, Appl. Phys. Lett. **50**, 1455 (1987).
[4]Y. Honda, S. Hosaka, A. Kikugawa, S. Tanaka, Y. Matsuda, M. Suzuki, and M. Futamoto, Jpn. J. Appl. Phys. **31**, L1061 (1992).
[5]J. F. Smyth, S. Schultz, D. R. Fredkin, T. Koehler, I. R. McFaydlin, D. P. Kern, and S. A. Rishton, J. Appl. Phys. **63**, 4237 (1988).
[6]G. A. Gibson, J. F. Smyth, S. Schultz, and D. P. Kern, IEEE Trans. Magn. **27**, 5187 (1991).
[7]R. M. H. New, R. F. W. Pease, and R. L. White, J. Vac. Sci. Technol. B **13**, 1089 (1995).
[8]R. M. H. New, R. F. W. Pease, R. L. White, R. M. Osgood, and K. Babcock, 40th MMM Conf.
[9]S. Y. Chou and P. Fischer, J. Vac. Sci. Technol. B **8**, 1919 (1990).
[10]P. B. Fischer, M. S. Wei, and S. Y. Chou, J. Vac. Sci. Technol. B **11**, 2570 (1993).
[11]S. Y. Chou, M. Wei, P. R. Krauss, and P. B. Fischer, J. Vac. Sci. Technol. B **12**, 3695 (1994).
[12]P. R. Krauss, P. B. Fischer, and S. Y. Chou, J. Vac. Sci. Technol. B **12**, 3639 (1994).
[13]L. Kong and S. Y. Chou (unpublished).
[14]S. Y. Chou and L. Kong (unpublished).
[15]P. R. Krauss and S. Y. Chou, J. Vac. Sci. Technol. B **13**, 2850 (1995). [16]S. Y. Chou and P. R. Krauss, presented at the 40th MMM Conf. Philadelphia, PA, Nov. 1995.
[17]U. Suriono and S. Y. Chou (unpublished).
[18]S. Y. Chou, P. R. Krauss, and P. Renstrom, Appl. Phys. Lett. **67**, 3113 (1995).
[19]L. F. Shew, IEEE Trans. Broadcast Tel. Receivers **BTR-9**, 56 (1963). [20]S. E. Lambert, I. L. Sanders, A. M. Patlach, and M. T. Krounbi, IEEE Trans. Magn. **MAG-23**, 3690 (1987).
[21]K. A. Belser, T. Makansi, and I. L. Sanders, U.S. Patent No. 4,912,585, March 27, 1990.
[22]S. E. Lamber, I. L. Sanders, A. M. Pattan, M. T. Krounbi, and S. R. Hetzler, J. Appl. Phys. **69**, 4724 (1991).